YF-16 Air Induction System Design Loads Associated with Engine Surge

Philip J. Evans* and Philip P. Truax†
General Dynamics, Fort Worth, Texas

Basic data and procedures used by the Fort Worth Division of General Dynamics Corporation to calculate structural loads due to engine surge on its YF-16 prototype fighter are presented. The procedure is based on a correlation of transient-pressure vs engine-compressor pressure ratio and relies heavily on extensive flight-measured transient-pressure data from engine-surge events on F-111 aircraft equipped with Pratt and Whitney TF30 family engines. These data were supplemented and confirmed by theoretical calculations for the YF-16 and by test-cell measurements of transient-pressure data from engine-surge events on the Pratt and Whitney F100-PW-100 engine, which is used in the YF-16.

Nomenclature

A = flow area
BPR = bypass ratio
F_{WS} = hammershock wave shape factor
K = $\Delta P_{HS}/P_2 M_2^{1.26}$
M = Mach number
m = mass flow
P = absolute pressure
T = temperature
t = time
V_H = level-flight maximum design speed for continuous operation
Δm = mass flow reduction in guillotine analogy
ΔP = differential pressure
ΔP_{HS} = incremental static pressure due to engine-surge-induced hammershock

Subscripts

0 = freestream
2 = engine face
4 = compressor exit
t = total conditions
SS = steady conditions

Introduction

THIS paper is primarily concerned with the prediction by the Fort Worth Division of General Dynamics of the potential air-induction system loads that could be created by engine surges on its YF-16 Lightweight Fighter (Fig. 1). The YF-16 is a prototype air-superiority day-fighter in which high performance, maximum maneuverability, low weight, and low cost are emphasized. It is powered by a Pratt and Whitney F100-PW-100 engine (for brevity, referred to as the F100). It is identical to that used in the F-15. A normal-shock inlet is used. When General Dynamics won the competition to design and build two prototypes of the YF-16, one of the problems faced was to determine the design loads on the air-induction system quickly and at minimum cost consistent with the low-cost philosophy of the prototype YF-16 program. This was not a serious problem since General Dynamics had on hand flight test measurements of engine-surge pressures for the F-111 with TF30 series engines.[1] Thus, for YF-16 surge load prediction, only two key issues needed resolution: 1) the effect of a new engine series on the strength of the surge for a given compressor pressure ratio, and 2) the effect of a duct with a different area variation on surge-wave propagation. (For a turbofan engine, "compressor pressure ratio," as used in this paper, means the overall compression ratio.) The first issue was resolved by examination of a limited amount of new engine-face surge data from the F100 engine that were obtained in a test cell with an airplane inlet attached. The second issue was resolved by reviewing the literature[2,3] and performing an analytical study, using a NASA computer program,[4] of unsteady flow in the YF-16 duct.

Received August 21, 1974; revision received January 27, 1975.
Index categories: Aircraft Structural Design (Including Loads); Airbreathing Engine Testing; Airbreathing Propulsion, Subsonic and Supersonic.

*Senior Structures Engineer, Fort Worth Division.
†Propulsion Group Engineer, Fort Worth Division. Member AIAA.

Engine Surge Phenomena

An engine surge can be described as a sudden reduction in flow in the compressor caused by abrupt flow breakdown or aerodynamic stalling of the blades in a portion of the compressor. This sudden reduction in flow creates a strong shock wave, frequently referred to as a hammershock, which moves upstream through the primary duct as illustrated in Fig. 2. This shock wave is the source of the high peak pressures that are the subject of this paper.

An engine surge is analogous to the sudden insertion of a guillotine into the flow in a duct, thus creating an abrupt reduction in the flow. A porous guillotine or one with downstream translation gives less than 100% flow reduction and is analogous to incomplete blockage in the compressor. Upstream air injection or upstream translation of the guillotine gives additional flow reduction and is analogous to the release of the stored energy in the compressor. The curves in Fig. 3 show the pressure rise for vaious flow-reduction ratios, $\Delta m/m$, in a constant-area duct. The flow is completely stopped when $\Delta m/m$ is equal to one. The pressure rise is seen to increase with initial duct Mach number, M_2, which is strictly equivalent to engine corrected airflow, and with the amount of flow reduction at the guillotine. This suggests that the pressure rise induced by an engine surge would depend on both the compressor pressure ratio and on the engine corrected airflow (or engine-face Mach number). Now, while this may

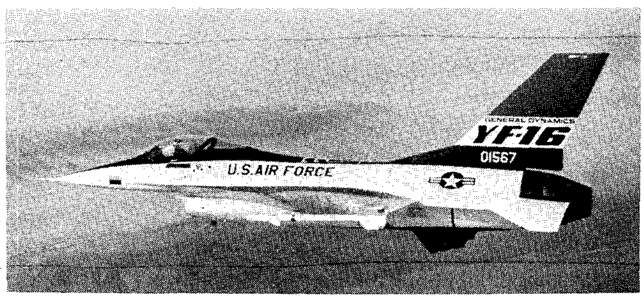

Fig. 1 YF-16 lightweight fighter.

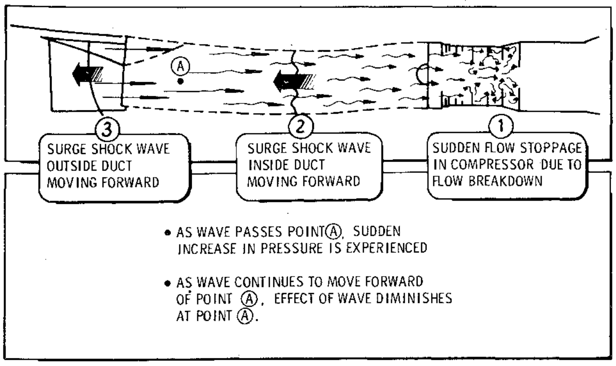

Fig. 2 Description of engine surge.

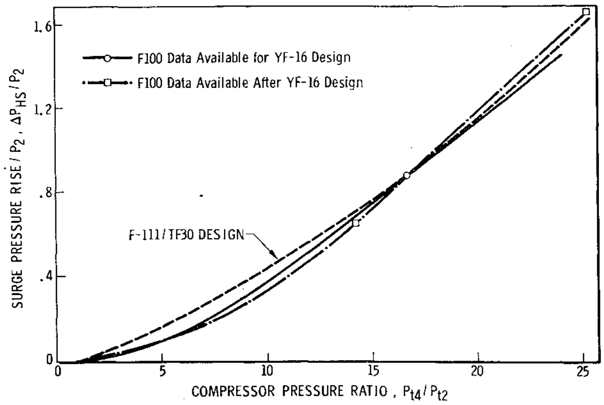

Fig. 4 Comparison of engine-face surge data for F-111/TF30 and F100.

be true in general, for a particular engine or compressor, at least over most of its operating range, the compressor pressure ratio correlates well with the corrected airflow on a one-to-one basis for normal operation. For such an engine, the surge pressure data would be expected to correlate well with either the compressor pressure ratio or the engine-face Mach number. Any departure from the one-to-one correspondence between corrected airflow and compressor pressure ratio (which could occur when the engine is limited by compressor discharge pressure) would be expected to be a source of scatter. For this reason alone, surge pressure correlations obtained from one engine series will not necessarily apply to a different engine series. If two engine series have nearly the same variation of compressor pressure ratio with engine-face Mach number, they would be more likely to generate the same surge pressure at a given compressor pressure ratio if other parameters are comparable.

Engine-Surge Basic Data

F100 Engine-Face Data

The surge pressure data from the F100 engine that have been furnished General Dynamics by the engine manufacturer are shown in Fig. 4. These data were obtained at the engine face in a test cell with a typical two-dimensional supersonic inlet attached to the engine. The solid curve, defined by only one data point (the circular symbol), constituted the only F100 surge data available for design. The two additional data points (the square symbols), which were received after the design was completed, provided the basis for the slightly revised fairing of F100 surge data. For comparison, the surge-data correlation for the engine face that was used for design of the F-111 with TF30 series engines is also included in Fig. 4.

The F-111/TF30 and the F100 surge data thus appeared to agree well at the engine face. This agreement and the scarcity of F100 data made it desirable to consider using the more plentiful and comprehensive F-111/TF30 data, which is to be described in more detail.

F-111/TF30 Data

The engine-surge basic data used for design of the production versions of the F-111 were obtained from flight test measurements by General Dynamics on several prototype F-111 airplanes. A summary of the inlet pressure instrumentation used to obtain the basic surge pressure data is presented in Fig. 5. Most of the pressure transducers were flush-mounted, with a frequency response which varied between 160 and 220 Hz.

The translating cowl on F-111A 12 was the most completely instrumented part of the air induction system for surge-load purposes. Data that show the distribution of steady and peak surge differential cowl pressures are shown in Fig. 6 for a typical surge. Data of this type were obtained for 24 hard surges over the Mach range from 0.76 to 2.09. A study of plots of peak surge pressure rise vs cowl station indicated that the assumption of a uniform peak surge pressure rise in the cowl region was reasonable, hence, it was decided to average the pressure rises from the 15 ΔP transducers. The resulting average incremental cowl pressure divided by the engine-face total pressure is correlated with compressor pressure ratio in Fig. 7. The fairing through the data points was used for F-111 design loads in the cowl region.

The longitudinal distribution of peak surge pressure rise for the entire inlet is shown in Fig. 8 relative to the average peak pressure rise in the cowl. This distribution was

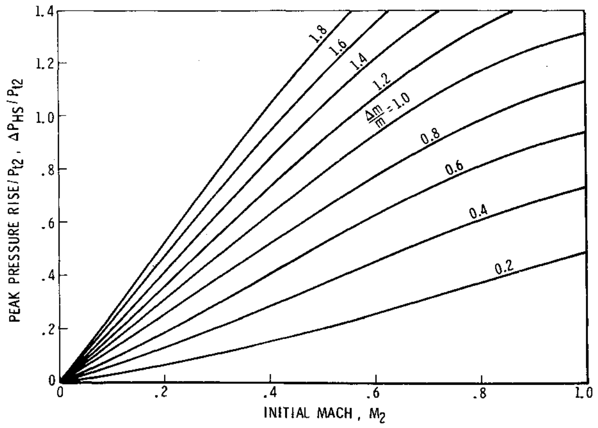

Fig. 3 Guillotine analogy of engine surge.

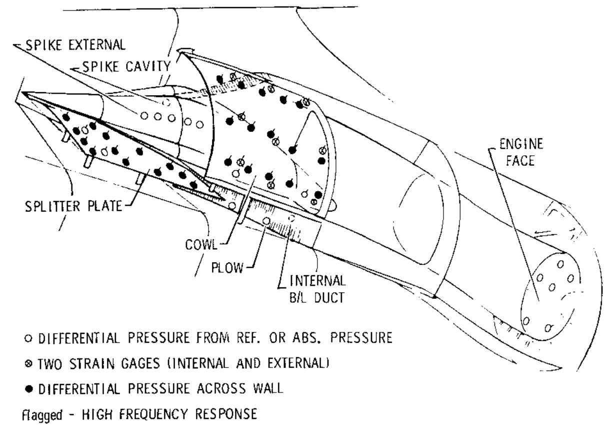

Fig. 5 F-111 flight test pressure instrumentation used to develop inlet pressure loads.

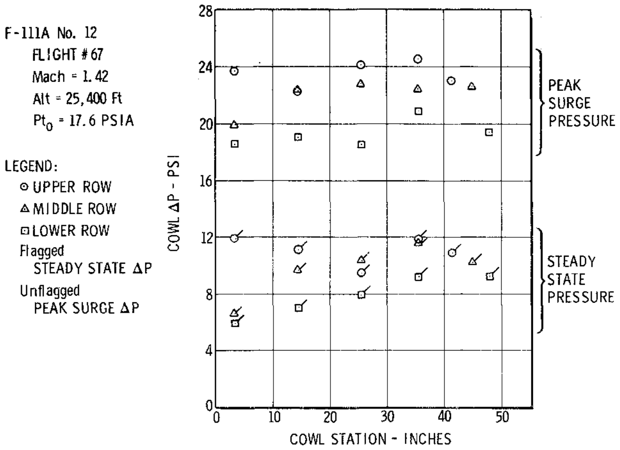

Fig. 6 Typical distribution of surge pressures in F-111 cowl.

determined as follows: Splitter-plate data from F-111A 13 were used to correlate the magnitude of peak surge pressure rise just forward of the cowl lip with the compressor pressure ratio, as was done for the cowl data. The resulting correlation was 90% of the cowl correlation fairing of Fig. 7. The splitter-plate surge data were also used to determine an average rate of decrease of peak surge rise forward of the cowl lip to be used for all surges. The resulting basic splitter-plate distribution is included in Fig. 8 as that part of the distribution forward of the cowl lip. This figure also shows a peak surge rise at the engine face of about 85% of that in the translating cowl area. This means that the cowl rise is about 18% greater than the engine-face rise. This number is based on analysis and correlation of surge pressure data measured at the engine face of F-111A 14 during inlet development testing.

There was concern that, if a surge load distribution similar to this distribution were used as the pressure rise distribution through the inlet at any instant of time, it would be unnecessarily conservative. This conservatism would exist if the values of this distribution did not occur simultaneously but rather, represented peaks of a traveling wave whose effect diminishes at a given point in the duct as the wave moves forward of that point. An attempt to determine the longitudinal shape of the traveling wave was made by comparing the time histories from transducers at different longitudinal locations. The resulting wave shapes deduced from splitter-plate and cowl surge oscillograph data are shown in Fig. 9. The upper curve applies to the duct aft of the cowl lip; the lower curve applies to the inlet stream tube forward of the cowl lip. For design purposes, it was assumed that these shapes could be used in conjunction with the peak surge distribution in Fig. 8 to obtain an instantaneous distribution of surge pressure rise for any location of wave front.

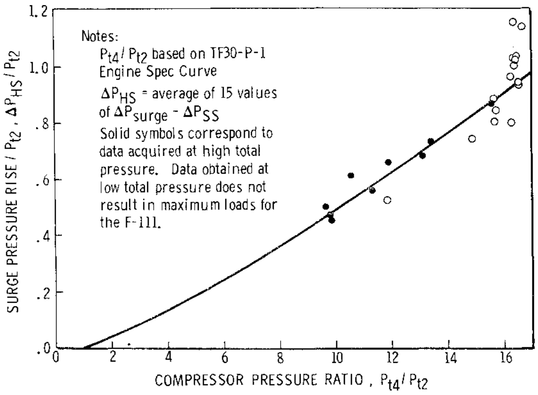

Fig. 7 F-111A cowl average surge pressure rise.

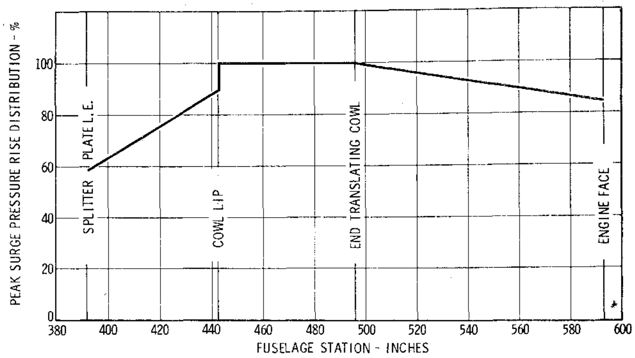

Fig. 8 F-111 peak surge pressure-rise distribution (relative to cowl peak pressure rise).

Subsequent Comparisons with Other Data Sources

It is useful to try to compare the F100 and F-111/TF30 surge data with some of the data from other data sources. Marshall[2] compared data from several sources by use of the surge parameter $K = \Delta P_{HS}/P_2 M_2^{1.26}$, which may be more general than other parameters since it enables the effects of compressor pressure ratio and M_2 (for just forward of the hub) to be separated. It is noted that, if an engine can have two operating points at the same compressor pressure ratio with different engine-face Mach numbers, a correlation of this type will yield a higher estimated surge pressure rise for the point having the higher engine-face Mach number. In Fig. 10, this parameter is used to compare the F-111/TF30 design engine-face correlation with the latest F100 data shown in Fig. 4. Engine-face data presented by Marshall for the TF30, which are based on data that he obtained by private communication from the NASA Flight Research Center (and which were later reported by Nugent and Holzman[5]), are also included, together with his theoretical estimate for the TF30 bypass ratio. His estimate agrees very well with these TF30 data from NASA, which are seen to be significantly less than the F-111/TF30 design data. Bellman and Hughes[6] also worked with NASA F-111/TF30 surge data from the Flight Research Center. These data, also shown in Fig. 10, were converted to the K parameter with the aid of approximate estimates of the Mach number just forward of the hub. They are seen to be considerably higher at the higher compressor pressure ratios than the other TF30 data when compared on this basis. The reason why the three sets of TF30 surge data differ is not known and may deserve further investigation.

Effects of Duct Geometry

Any of the curves of Fig. 4 appeared to provide an acceptable engine-face surge pressure correlation for the

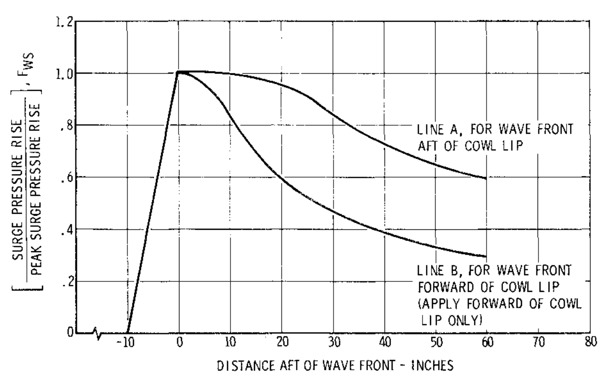

Fig. 9 F-111 surge pressure-rise wave shapes.

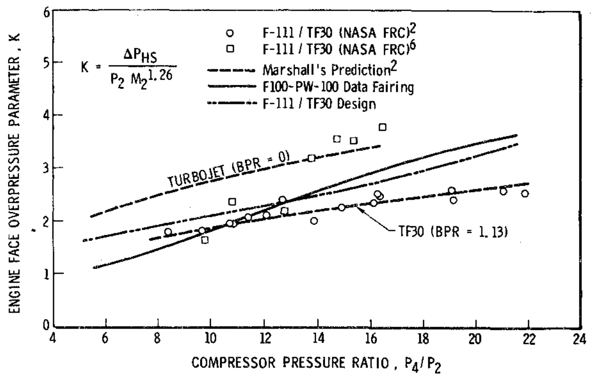

Fig. 10 Comparison of surge data using Marshall's parameter.

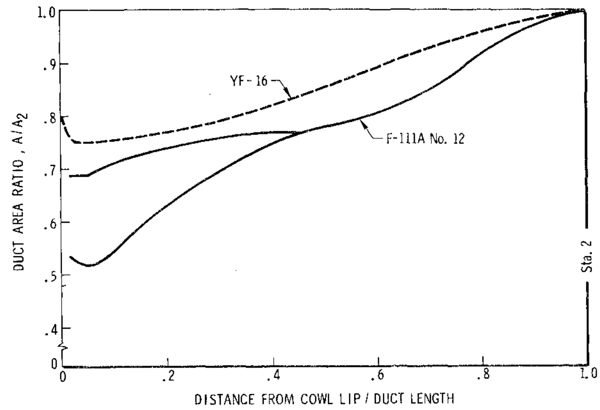

Fig. 12 Comparison of duct contraction for YF-16 and F-111.

F100 engine for the airplane inlet it was tested with. However, no information was available on the area distribution of the inlet used, which was not the YF-16 configuration. This possible difference in ducts caused some concern because calculated results by Mays[3] for a 100% impulsive flow stoppage (Fig. 11) showed a big increase in hammershock pressure rise at the engine face as the amount of contraction increased. But it was not clear that the Mays results would be valid for the actual airflow time history during an engine surge.

An estimate of the contraction of the YF-16 inlet showed it to be relatively small (Fig. 12) and, therefore, probably not significantly greater than for the inlet used with the F100 when the surge data were obtained. Therefore, it was decided that the F100 engine-face data did not need to be corrected for contraction-ratio differences. However, since the F-111/TF30 correlation is slightly more conservative than the initial F100 correlation, it was selected for design of the YF-16.

Another question associated with duct contraction is its effect on the surge pressure rise upstream of the engine face. Again, Mays, using the impulsive flow-stoppage model for a mixed compression inlet with a throat area equal to half the engine-face area, predicted a surge static pressure rise near the throat approximately 76% greater than the rise at the engine face. On the other hand, Choby and others[7] report surge data that show approximately a 9% decrease in the static-pressure rise at the throat relative to the engine face. It was decided that the 18% increase for the cowl pressure rise over the engine-face pressure rise that was used for the F-111 would probably be more reasonable than a higher value based on the Mays analysis. It was reasoned that the use of an 18% increase for the YF-16 could very well be slightly conservative because of the higher contraction in the F-111 duct (Fig. 12). This conclusion was supported by surge-wave propagation calculations for the YF-16 duct geometry made with the NASA procedure developed by Matthews.[4] The resulting variation of peak surge pressure rise with axial location in the duct showed the peak rise at the cowl lip to be almost as high as indicated by the F-111 design data.

YF-16 Design Data Summary

The intensity and distribution of the surge pressure-rise data that were selected for YF-16 design are summarized in Figs. 13 and 14. These curves represent the same data that were used for F-111 design, as explained in the foregoing discussion, except that the axial distribution in the duct has been simplified by the use of a single straight line from the engine face to the cowl lip.

Load Calculation Approach and Results

The basic elements that enter into a surge load calculation are the peak surge-pressure-rise correlation of Fig. 13, the freestream total pressure and temperature (which are a function of flight condition and model atmosphere), the inlet pressure recovery, and the compressor pressure ratio. Design surge-load estimates for cold, standard, and hot model atmospheres are required to satisfy the structural criteria. The compressor pressure ratio is usually obtained as output from a computer program supplied by the engine manufacturer with the foregoing information as part of the input. Minimum power extraction and minimum compressor bleed are assumed to maximize P_{t4}. Also required are the distribution of peak surge pressure rise and the wave shapes, if this refinement is warranted. The resulting distribution of surge pressure rise is superimposed

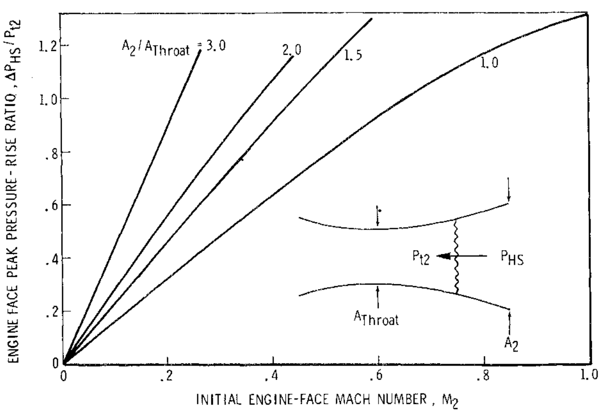

Fig. 11 Effect of duct contraction for impulsive flow stoppage (from Mays[3]).

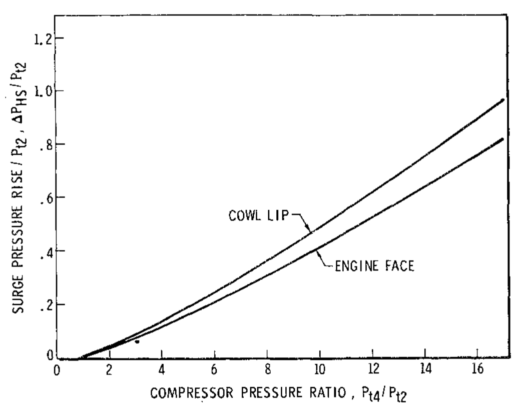

Fig. 13 YF-16 design surge pressure data.

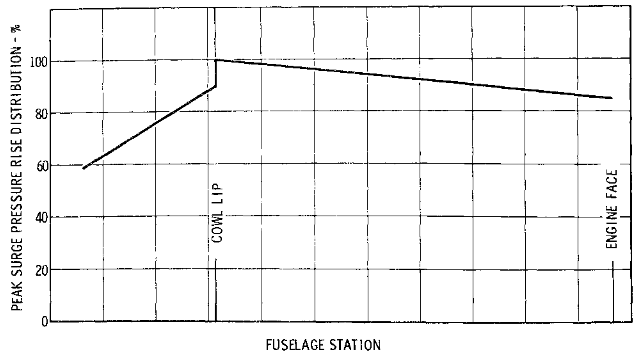

Fig. 14 YF-16 peak surge pressure-rise distribution (relative to cowl peak pressure rise).

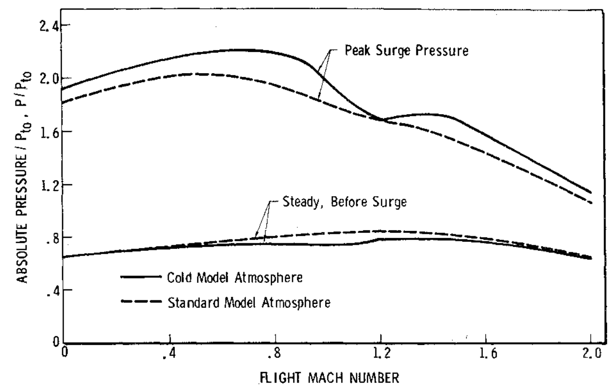

Fig. 15 YF-16 forward duct pressures at V_H.

on the distribution of steady pressure just before the surge. This study-pressure distribution is a function of the engine corrected airflow just before the surge. The resulting values along the V_H line of average peak surge and steady pressure (divided by P_{to}) in the forward duct are shown in Fig. 15 for cold and standard model atmospheres. The highest surge pressures are associated with the cold model atmosphere because of the resulting higher corrected airflow and compressor pressure ratio. It should be noted that an assumption cannot be made that the critical surge loads will automatically occur on the design speed line. Higher loads could occur at lesser speeds where the engine is limited by compressor discharge pressure.

It is also necessary to specify the engine surge pressure on the splitter plate and fuselage panels forward of the inlet. For the splitter plate, the portion of the peak surge-pressure-rise distribution (Fig. 14) forward of the inlet was used. For the fuselage panels, that part of the curve of Fig. 14 forward of the cowl lip was lowered somewhat because of the greater separation distance of the fuselage panels from the inlet stream tube and also because of interaction with the thicker boundary layer on the fuselage. The data were also extrapolated forward to the rear end of the radome, which was conservatively assumed to be the forward limit of the surge shock wave. The surge wave shape of Fig. 9 was also superimposed. This fairly arbitrary procedure was believed to be conservative for fuselage panel design. More and better data on the effect of engine surges on the panels forward of inlets are clearly needed.

Conclusions

Extensive data from flight testing of F-111 aircraft equipped with Pratt and Whitney TF30-series turbofan engines were used to establish design distributions of engine-surge pressure inside and forward of the F-111 inlet duct and to correlate surge-pressure magnitude with compressor pressure ratio. Sufficient test-cell engine-face surge-pressure data were available from the Pratt and Whitney F100-PW-100 engine used in the YF-16 lightweight fighter to establish, by comparison with the F-111/TF30 engine-face surge data, that the surges generated by the two engines at the same compressor pressure ratio have nearly equal strengths. This agreement, together with similarities of duct geometry, justified the use of General Dynamics' more extensive F-111/TF30 data in conjunction with F100 compressor pressure ratios for the determination of YF-16 inlet design loads.

Because the F100 engine was selected by General Dynamics when it was well along in its development, sufficient supporting surge data were available on the F100 from Pratt and Whitney when needed for YF-16 inlet design surge-load predictions. To facilitate the timely determination of design surge loads for future programs, especially those wherein engine development is concurrent with airplane design, it is recommended that accurate engine-face surge-pressure data be routinely collected and published by engine manufacturers and government laboratories doing engine research.

References

[1]Barnard, J. D. and Evans, P. J., "Air Induction System Engine Stall Loads," *Proceedings of the Third Structural Loads Workshop for Preliminary Aerospace Design Projects,* Aeronautical Systems Division, Wright-Patterson Air Force Base, Ohio, 1970, pp. 89–127.

[2]Marshall, F. L., "Prediction of Inlet Duct Overpressures Resulting from Engine Surge," *Journal of Aircraft,* Vol. 10, May 1973, pp. 274–278.

[3]Mays, R. A., "Inlet Dynamics and Compressor Surge," *Journal of Aircraft,* Vol. 8, April 1971, pp. 219–226.

[4]Matthews, C. W., "Numerical Study of Control of Dynamic Properties of a Supersonic Inlet Using Bypass Bleed," TN D-6144, Jan. 1971, NASA.

[5]Nugent, J. and Holzman, J. K., "Flight-Measured Inlet Pressure Transients Accompanying Engine Compressor Surges on the F-111A Airplane," TN D-7696, June 1974, NASA.

[6]Bellman, D. R. and Hughes, D. L., "The Flight Investigation of Pressure Phenomena in the Air Intake of an F-111A Airplane," AIAA Paper 69-488, U.S. Air Force Academy, Colo., 1969.

[7]Choby, D. A., Burstadt, P. L., and Calogeras, J. E., "Unstart and Stall Interactions Between a Turbojet Engine and an Axisymmetric Inlet with 60-Percent Internal-Area Contraction," TM X-2192, March 1971, NASA.